Static and dynamic analysis of plates of arbitrary shape and boundary condition

Static and Dynamic Analysis of Plates of Arbitrary Shape and Boundary Condition

Etude statique et dynamique des plaques de forme et de conditions au contour quelconques

Statische und dynamische Berechnung von Platten willkürlicher Form und Randbedingungen

RUDOLPH SZILARD
Dr. Ing., Professor of Civil Engineering, Senior Research Engineer, University of Denver, Denver, Colorado

WILLIAM F. HUBKA
Research Engineer, University of Denver, Denver, Colorado

I. Introduction

The prevailing tendency in modern structural engineering is to use lighter, and thus more economical, structures. Utilization of the two-dimensional load carrying capacity inherent to plates satisfies the requirements of this modern trend to a great extent and explains the frequent use of these structural elements in the fields of aeronautical, civil, mechanical and marine engineering. In addition to the academic interest, the pressing economic needs of the above-mentioned engineering areas require solution of complex plate problems such as plates of arbitrary shape and boundary condition subjected to arbitrary static or dynamic loads. The analysis of such problems by means of classical methods [1] is time consuming, requires extensive mathematical background, and in many cases is quite impossible due to the associated mathematical difficulties. Although the finite difference method can be successfully employed in nearly any problem [2], the solution of complex plate problems by this method is generally economically undesirable.

In the following, an improved discrete element and stiffness matrix approach to complex plate problems is presented [3]. This solution makes extensive use of modern electronic computers with the method for complete automation is outlined. For the discrete element, a square plate element has been choosen. The "nodal" points, where continuity is expressed, are located at the centers

of the fixed edges (Fig. 1). The usual assumptions of elastic plate theories [2] considering small deflections have been used to obtain the elements of the stiffness matrix.

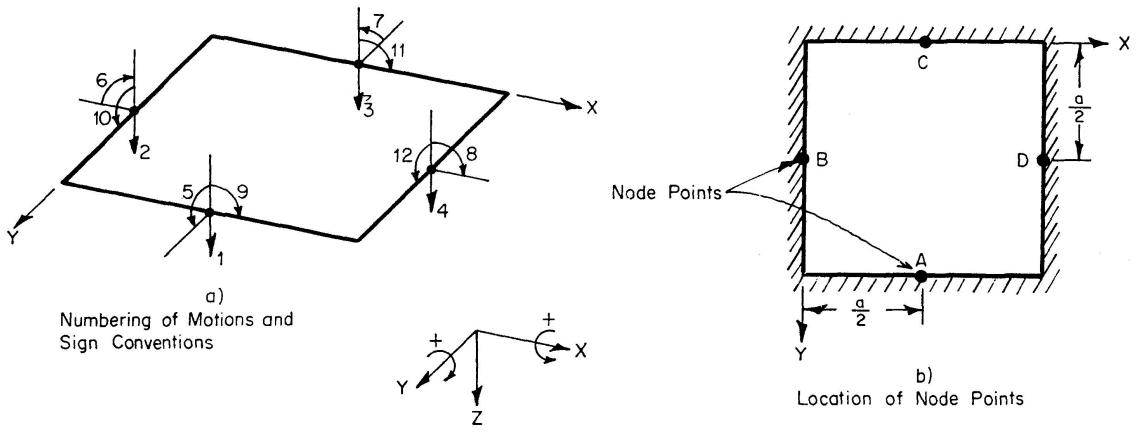

Fig. 1. Discrete element.

II. Matrix Formulation of Static and Dynamic Plate Problems

Any static structural problem (plates are no exception in this respect) can be expressed by the following matrix equation [5]:

$$\{x_i\} = [\delta_{ij}]\{P_j\}, \tag{1}$$

where $\{x_i\}$ represents the column matrix of the displacement components (translation or rotation), $[\delta_{ij}]$ is the flexibility matrix of the structure, and $\{P_j\}$ is the column matrix of the loads (force or moment).

In the case of plates subjected to transverse loading, Eq. (1) becomes:

$$\{w_i\} = [\delta_{ij}]\{P_j\}, \tag{1a}$$

where w_i denotes the lateral deflection of the plate.

Utilizing the important relationship [6] which exists between the flexibility matrix $[\delta_{ij}]$ and stiffness matrix $[\rho_{ij}]$:

$$[\delta_{ij}] = [\rho_{ij}]^{-1}, \tag{2}$$

Eq. (1a) becomes:

$$\{w_i\} = [\rho_{ij}]^{-1}\{P_j\}. \tag{3}$$

If the load is a function of time t the matrix equation of motion has the following form:

$$\{w_i\} + [\rho_{ij}]^{-1}\{m_i \ddot{w}_i\} = [\rho_{ij}]^{-1}\{P_j(t)\}, \tag{4}$$

where m_i represents the lumped mass at point "i", and the two dots denote differentiation with respect to time $\left(\frac{\partial^2 w}{\partial t^2}\right)$.

In the case of free vibration, Eq. (4) becomes:

$$\{w_i\} + [\rho_{ij}]^{-1}\{m_i \ddot{w}_i\} = 0 \tag{5}$$

or, using Navier's "forced" solution in form of:

$$w_i = W_i \cos \omega t \quad \text{or} \quad w_i = W_i \sin \omega t. \tag{6}$$

Eq. (5) is transformed into:

$$[\rho_{ij}]\,[m_i]^{-1} - \omega^2 I = 0 \tag{7}$$

representing the classical eigen-value problem of linear algebra [7] in the form of:

$$A - \lambda I = 0, \tag{8}$$

where I denotes the unit matrix and A is the "dynamic matrix".

In addition to the natural circular frequencies ω, Eq. (8) yields the modes of free vibrations in the form of eigenvectors [7].

Expressing the arbitrary (in time) load in Fourier Series by appropriate selection of the period of expansion [8] and by suitable arbitrary continuation of its load versus time curve (Fig. 2), the load can be expressed conveniently in either sine or cosine terms; thus:

$$P_j = \sum_n \mathfrak{P}_{jn} \sin p t, \tag{9}$$

where $p = \frac{n\pi}{T}$ is the circular frequency of the load.

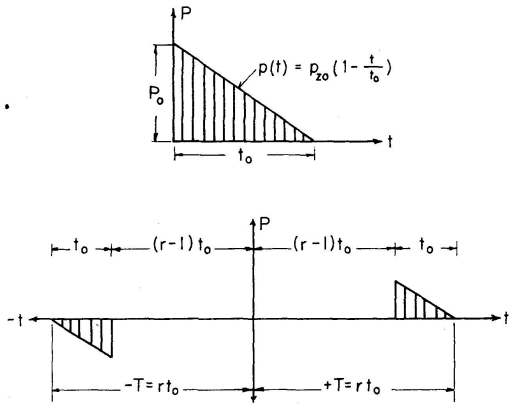

Fig. 2. Arbitrary extension of non-periodic load for Fourier series expansion (sine terms only).

If the deflection w_i is expressed in a form similar to that of the load:

$$w_i = \sum_n \mathfrak{W}_{in} \sin p t, \tag{10}$$

the differential equation of motion (4) is transformed again into a series of algebraic equations with the unknowns $\mathfrak{W}_{in}$. Adding the free vibration to the forced one, the complete dynamic response of the plate is obtained.

The above-outlined solutions for structures of general type are well documented in the pertinent literature [5] and [6] and "ready made" computer programs are available in "Computer Centers" eliminating tedious programing and contributing considerably to the economy of the method.

Knowing the vertical deflection $w(x, y)$ of the plate, the internal forces and moments can be obtained [2]. Thus the key to the matrix solution of complex static or dynamic plate problems is the determination of the stiffness matrix $[\rho_{ij}]$. The use of the stiffness matrix as opposed to flexibility or transfer matrices [9], [10] offers the following significant advantages [11]:

a) The structure can be disassembled: thus, the effects are localized. The stiffness matrix of the total structure is easily obtained by simple algebraic addition of the overlapping elements.

b) The resulting matrix is positive-definite and symmetrical, offering additional advantages in computer solutions.

c) Any boundary condition can be considered with relative ease.

III. Determination of Improved Stiffness Matrix

There have been numerous attempts in the past ([12], [13], [14], [15] etc.) to utilize the discrete element approach to the solution of plate problems. The basic philosophy underlying the method presented here is that, by improving the stiffness matrix coefficients, higher accuracy coupled with greater economy can be achieved.

In order to obtain the stiffness matrix $[\rho_{ij}]$, of the plate, the structure is first disassembled into finite ($\Delta x = a$, $\Delta y = a$) square discrete elements. Next, the coefficients of the stiffness matrix for each discrete element are determined; then, the stiffness matrices of the discrete elements are compiled into the stiffness matrix of the entire plate considering various boundary conditions.

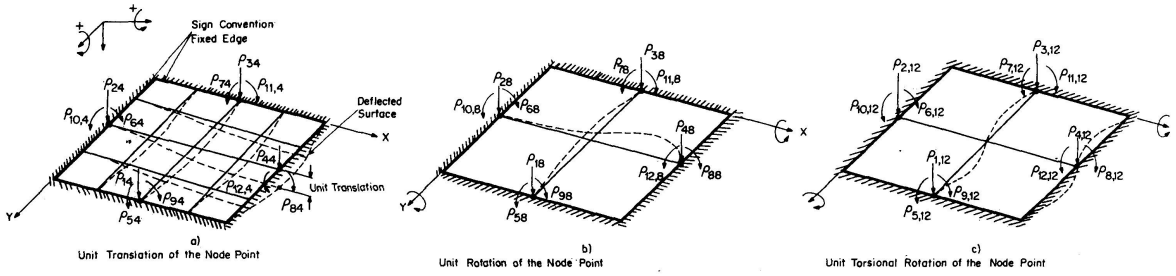

Fig. 3. Unit motions of the node points.

The determination of the coefficients for the stiffness matrix of the discrete element may be accomplished in the following manner. According to the definition of the stiffness matrix [11], the node "D" (Fig. 1) is subjected to unit translations and unit rotations (one at the time) while motions at the other node points are prevented by keeping the edges fixed (Fig. 3). These unit motions produce forces and moments along all edges; the forces and moments are then integrated along the edge and the statically equivalent resulting

forces and moments are placed at the node points, thereby yielding the elements of the stiffness matrix of the discrete plate element.

The differential equation of elastic plates with flexural rigidity having small deflections due to transverse loads [2]:

$$\frac{\partial^4 w}{\partial x^4}+2\frac{\partial^4 w}{\partial x^2\partial y^2}+\frac{\partial^4 w}{\partial y^4}=\frac{p_z(x,y)}{D} \tag{11}$$

has been expressed in finite difference form (Fig. 4):

$$20\,w_0-8\,(w_1+w_2+w_3+w_4)+2\,(w_5+w_6+w_7+w_8)+w_9+w_{10}+w_{11}+w_{12}=\lambda^4\frac{(P_z=1)}{D}, \tag{12}$$

where D represents the flexural rigidity

$$D=\frac{E\,h^3}{12\,(1-\mu^2)} \tag{13}$$

of the plate, E denotes the Young's modulus, h the plate thickness, and μ the Poisson's ratio. Since, in elastic theory, the displacement w is proportional to the force:

$$\frac{P_z^{\mathrm{I}}=1}{w^{\mathrm{I}}}=\frac{P_z^{\mathrm{II}}=\rho}{w^{\mathrm{II}}=1}, \tag{14}$$

this relationship gives the scaling law, which must be applied to obtain the forces and moments along the edges which are created by unit motion.
In the same manner, the edge moments can be expressed in finite difference form:

$$\begin{aligned} M_x&=\frac{-D}{\lambda^2}[(w_1-2\,w_0+w_3)+\mu\,(w_2-2\,w_0+w_4)],\\ M_y&=\frac{-D}{\lambda^2}[(w_2-2\,w_0+w_4)+\mu\,(w_1-2\,w_0+w_3)]. \end{aligned} \tag{15}$$

The total edge supporting reaction V_x is considered to be the sum of two components, Q_x and $\frac{\partial M_{xy}}{\partial y}$; thus:

$$V_x=Q_x-\frac{\partial M_{xy}}{\partial x}=-D\frac{\partial}{\partial x}\left[\frac{\partial^2 w}{\partial x^2}+(2-\mu)\frac{\partial^2 w}{\partial y^2}\right] \tag{16}$$

and, in similar manner:

$$V_y=Q_y-\frac{\partial M_{xy}}{\partial x}=-D\frac{\partial}{\partial y}\left[\frac{\partial^2 w}{\partial y^2}+(2-\mu)\frac{\partial^2 w}{\partial x^2}\right], \tag{17}$$

where M_{xy} represents the torsional moment [2]. In the case of fixed edges, however, the twisting moments are zero, making the revision of Eqs. (16) and (17) necessary. This revision may be accomplished in the following manner. The fourth order plate Eq. (11) may be replaced by two equations of the second order, each representing the deflection of a membrane. Thus:

$$\left(\frac{\partial^2}{\partial x^2}+\frac{\partial^2}{\partial y^2}\right)\overline{M}=-p_z \tag{18}$$

and

$$\left(\frac{\partial^2}{\partial x^2}+\frac{\partial^2}{\partial y^2}\right)w=-\frac{\overline{M}}{D}, \tag{19}$$

where $\overline{M}$ is defined by GIRKMANN [4] as the "Momentensumme" and is equal to:

$$\overline{M}=\frac{M_x+M_y}{1+\mu}. \tag{20}$$

The property of $\overline{M}$ is that it is invariant on the surface of the plate. GIRKMANN has shown that from the considerations of "the elastic web" the value of $\overline{M}$ may be uniquely determined everywhere on the plate. Then, by expressing the shear force Q in terms of $\overline{M}$, a unique expression can be derived for V_x and V_y:

$$V_x=V_y=-D\left(\frac{\partial}{\partial x}+\frac{\partial}{\partial y}\right)\overline{M}. \tag{21}$$

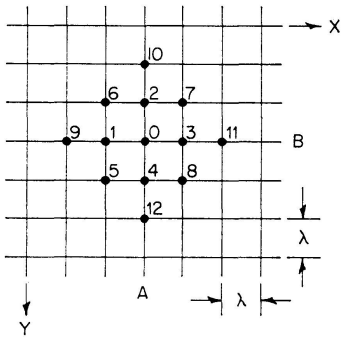

Fig. 4. Finite difference grid reference.

Using the lines A–A and B–B in Fig. 4 as fixed edges, Eq. (21) is written for point "0" as:

$$V_x=V_y=-\frac{D}{2\lambda^3}[20\,w_0-8\,(w_1+w_2+w_3+w_4)+2\,(w_5+w_6+w_7+w_8)+w_9+w_{10}+w_{11}+w_{12}]. \tag{22}$$

Due to symmetry, the gridwork of the finite difference solution of Eqs. (14), (15) and (22) need to be extended only to half of the discrete element (Fig. 5), or to one quadrant of an analytical model, such as Fig. 6.

The introduction of the analytical model in the form of a plate with edge lengths "a" and "$2a$" respectively yields the following advantages:

a) the results obtained from the finite difference solution could be checked against an available solution [2] using $P_z=\frac{1}{2}$ loading, and refined when required, and

b) the analytical model allows the introduction of moment by means of couples with relative ease.

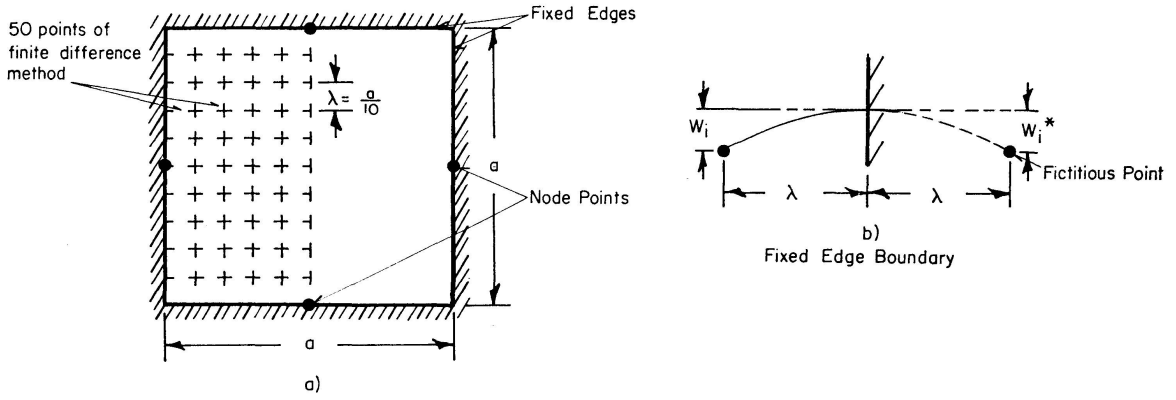

Fig. 5. Finite difference method.

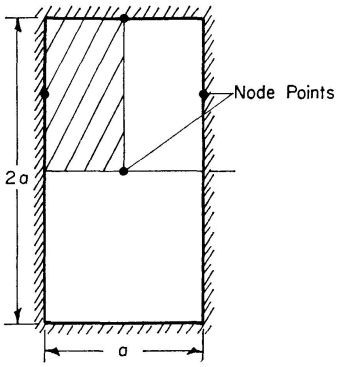

Fig. 6. Analytical model of discrete element.

The distribution of moments and edge reactions along the edge of the discrete element, due to each case of unit motion of the node point "A", is shown in Figs. 7 through 9. When this distribution is unsymmetrical with respect to the node points, the statically equivalent forces (resultant + moment) represent the required elements of the stiffness matrix.

When all the forces and moments have been calculated for a given unit motion, the plate, taken as a free body, is checked for static equilibrium by summation of forces and moments. In every case, the plate is found to be in equilibrium, and indication that the numerical analyses are correct[1]).

It has been mentioned that a further analytical check concerning the elements of the stiffness matrix of the discrete element is obtained by using the "rigorous" solution [2] of the deflected surface of a plate with fixed edge conditions, loaded with a centrally located concentrated load, having the edge dimensions "a" and "$2a$".

The rigorous solution of this problem uses a series solution and the law of superposition [2]. The surface of the deflected plate is given in the form of

$$w(x, y) = w_1 + w_2 + w_3, \tag{23}$$

where w_1 represents the deflection of the simply supported plate subjected to a concentrated load acting at the center of the plate; w_2 is the deflection of

[1]) Although the macroscopic equilibrium of stiffness coefficients given in Fig. 10 is violated, the solution converges very fast.

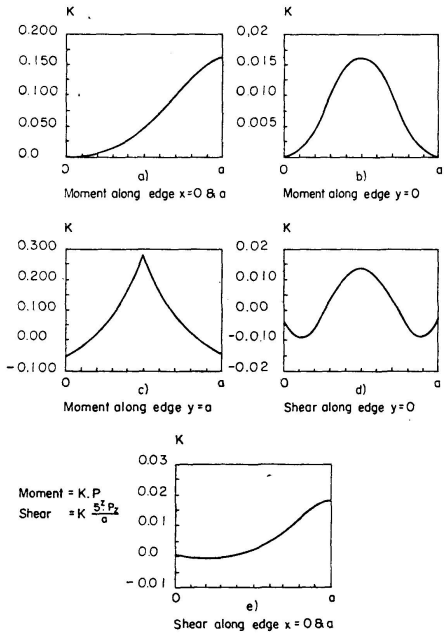

Fig. 7. Variation of moment and shear along fixed edges due to unit translation of node point.

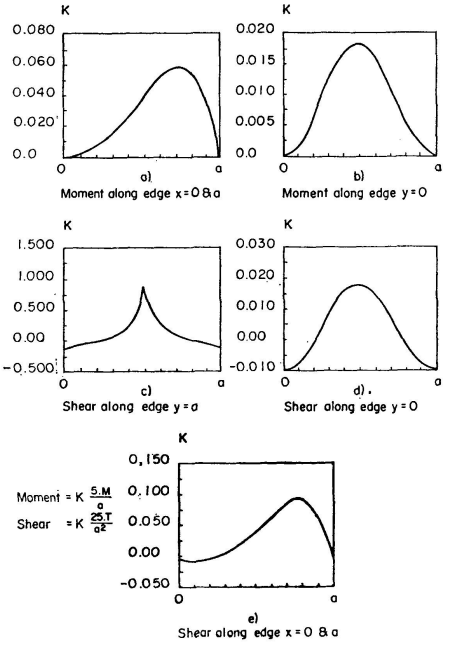

Fig. 8. Variation of moment and shear along fixed edges due to unit rotation of node point.

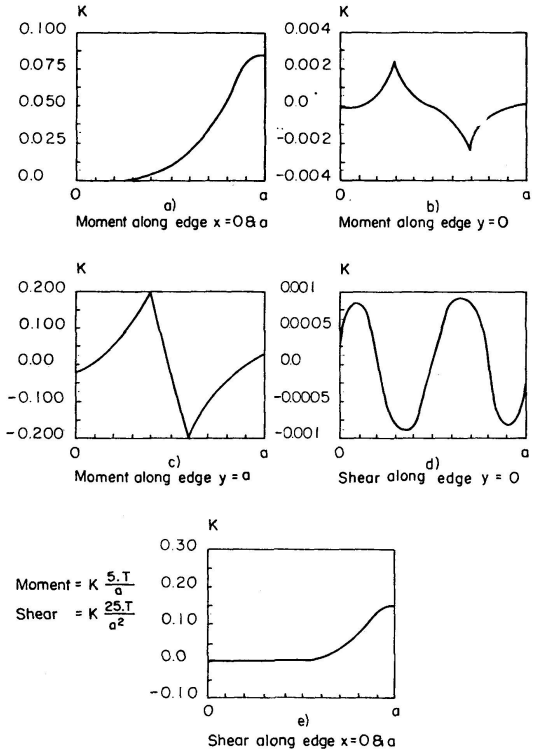

Fig. 9. Variation of moment and shear along fixed edges due to unit torsional rotation of node point.

the simply supported plate subjected to distributed moments along one pair of opposite edges; and w_3 is the deflection of the simply supported plate bent by moments acting along the other pair of edges.

The equation of w_1 is given as:

$$w_1 = \frac{P_z a^2}{2\pi^3 D} \sum_{m=1,3,\ldots} \frac{1}{m^3} \cos\frac{m\pi x}{a} \left[\left(\tanh\alpha_m - \frac{\alpha_m}{\cosh^2 a_m} \right) \cosh\frac{m\pi y}{a} - \sinh\frac{m\pi y}{a} - \tanh\alpha_m \frac{m\pi y}{a} \sinh\frac{m\pi y}{a} + \frac{m\pi y}{a} \cosh\frac{m\pi y}{a} \right]. \tag{24}$$

Expressions for w_2 and w_3 have the following forms:

$$w_2 = \tag{25}$$
$$-\frac{a^2}{2\pi^2 D} \sum_{m=1,3,\ldots} A_m \frac{(-1)^{\frac{m-1}{2}}}{m^2 \cosh\alpha_m} \cos\frac{m\pi x}{a} \left[\frac{m\pi y}{a} \sinh\frac{m\pi y}{a} - \alpha_m \tanh\alpha_m \cosh\frac{m\pi y}{a} \right],$$

$$w_3 = \tag{26}$$
$$-\frac{b^2}{2\pi^2 D} \sum_{m=1,3,\ldots} B_m \frac{(-1)^{\frac{m-1}{2}}}{m^2 \cosh\beta_m} \cos\frac{m\pi y}{b} \left[\frac{m\pi x}{b} \sinh\frac{m\pi x}{b} - \beta_m \tanh\beta_m \cosh\frac{m\pi x}{b} \right],$$

where $\alpha_m = \frac{m\pi b}{2a}$; $\beta_m = \frac{m\pi a}{2b}$ and $b = 2a$.

Assuming the edges of the plate to be located at $y = \pm\frac{b}{2}$ and $x = \pm\frac{a}{2}$, the edge moments are given by:

$$(m_y)_{y=\pm\frac{b}{2}} = \sum_{m=1,3,\ldots} (-1)^{\frac{m-1}{2}} A_m \cos\frac{m\pi x}{a},$$
$$(m_x)_{x=\pm\frac{b}{2}} = \sum_{m=1,3,\ldots} (-1)^{\frac{m-1}{2}} B_m \cos\frac{m\pi y}{b}. \tag{27}$$

The coefficients A_m and B_m are determined from the condition that the slope of the deflected surface at the edges is zero; that is, from the set of simultaneous equations defined by

$$\left(\frac{\partial w}{\partial y}\right)_{y=\pm\frac{b}{2}} = 0 \qquad \text{and} \qquad \left(\frac{\partial w}{\partial x}\right)_{x=\pm\frac{a}{2}} = 0. \tag{28}$$

Performing the indicated operations we obtain:

$$A_k \frac{1}{k} \left[\tanh\alpha_k + \frac{\alpha_k}{\cosh^2\alpha_k} \right] + \frac{8\alpha k}{\pi b} \sum_{m=1,3,\ldots} \frac{B_m}{m^3} \frac{1}{\left(\frac{a^2}{b^2} + \frac{k^2}{m^2}\right)^2} = -\frac{P_z (-1)^{\frac{m-1}{2}}}{\pi k^2} \frac{\alpha_k \tanh\alpha_k}{\cosh\alpha_k} \tag{29}$$

and

$$B_k \frac{1}{k} \left[\tanh\beta_k + \frac{\beta_k}{\cosh^2\beta_k} \right] + \frac{8bk}{\pi a} \sum_{m=1,3,\ldots} \frac{A_m}{m^3} \frac{1}{\left(\frac{b^2}{a^2} + \frac{k^2}{m^2}\right)^2} = -P_z \frac{(-1)^{\frac{m-1}{2}}}{\pi k^2} \frac{\beta_k \tanh\beta_k}{\cosh\beta_k}, \tag{30}$$

$$k = 1, 2, 3.$$

The final solution for A_m and B_m is made by forming a system of equations in matrix form by successively incrementing k and summing over m. The series is truncated at an arbitrary point, the matrix is inverted and the coefficients are calculated by multiplying the inverse matrix and the matrix of P coefficients. For example $k=1,3,5$, and $m=1,3,5$:

$$\begin{bmatrix} C_{A1} & 0 & 0 & C_{B1} & C_{B3} & C_{B5} \\ 0 & C_{A3} & 0 & C_{B1} & C_{B3} & C_{B5} \\ 0 & 0 & C_{A5} & C_{B1} & C_{B3} & C_{B5} \\ C_{A1} & C_{A3} & C_{A5} & C_{B1} & 0 & 0 \\ C_{A1} & C_{A3} & C_{A5} & 0 & C_{B3} & 0 \\ C_{A1} & C_{A3} & C_{A5} & 0 & 0 & C_{B5} \end{bmatrix} \begin{bmatrix} A_1 \\ A_3 \\ A_5 \\ B_1 \\ B_3 \\ B_5 \end{bmatrix} = \begin{bmatrix} C_{P1} \\ C_{P3} \\ C_{P5} \\ C_{P1} \\ C_{P3} \\ C_{P5} \end{bmatrix} P. \tag{31}$$

The upper half of the matrix is formed from the first equation and the lower half from the second.

C_{Ai}, C_{Bi} and C_{Pi} denote the numerical values calculated for A_i, B_i and P_i. When the coefficients A_m and B_m have been found, the reactions along the plate edge can be calculated.

The quantities of interest are:

1. Maximum central deflection.
2. Integrals of the moments along clamped edges and along the "guided" edge.
3. Integrals of shear forces along clamped edges.
4. Integrals of torsional moments along clamped edges.

The equations necessary for these calculations are given in final form:

$$\int_{-a/2}^{+a/2} m_y\,dx\Big|_{y=\frac{b}{2}} = \frac{2a}{\pi}\sum_m \frac{A_m}{m}, \tag{32}$$

$$\int_0^{b/2} m_x\,dy\Big|_{x=\frac{a}{2}} = \frac{2a}{\pi}\sum_m \frac{B_m}{m}, \tag{33}$$

$$\begin{aligned}\int_0^{b/2} m_y\,dx\Big|_{y=0} = {} & \frac{P_z a}{\pi^2}\sum_m \frac{(-1)^{\frac{m-1}{2}}}{m^2}\left[(1-\mu)\frac{\alpha_m}{\cosh^2\alpha_m}+(1+\mu)\tanh\alpha_m\right] \\ & +\frac{a}{\pi}\sum_m \frac{A_m}{\cosh\alpha_m}[2-(1-\mu)\alpha_m\tanh\alpha_m]-\frac{2a}{\pi}\sum_m \frac{B_m}{m}\cdot \\ & \cdot(-1)^{\frac{m-1}{2}}[(1-\mu)\beta_m-(1+\mu)\tanh\beta_m-(1-\mu)\beta_m\tanh^2\beta_m],\end{aligned} \tag{34}$$

$$\begin{aligned}\int_0^{b/2} Q_x\,dy\Big|_{x=\frac{a}{2}} = {} & -\sum_m \beta_m\tanh\beta_m+\sum_m A_m\tanh\alpha_m \\ & +\frac{P_z}{\pi}\sum_m \frac{(-1)^{\frac{m-1}{2}}}{m}[\tanh\alpha_m\sinh\alpha_m-\cosh\alpha_m+1],\end{aligned} \tag{35}$$

$$\int_{-a/2}^{+a/2} Q_y\,dx\Big|_{y=\frac{b}{2}} = \frac{2P_z}{\pi}\sum_m \frac{(-1)^{\frac{m-1}{2}}}{m}\left[\cosh\alpha_m - \tanh\alpha_m \sinh\alpha_m\right] - 2\sum_m A_m \tanh\alpha_m + 2\sum_m B_m \tanh\beta_m, \tag{36}$$

$$\int_0^{b/2} y\,Q_x\,dy\Big|_{x=\frac{a}{2}} = \frac{P_z a}{\pi}\sum_m \frac{(-1)^{\frac{m-1}{2}}}{m}\left[\sinh\alpha_m - \cosh\alpha_m + \frac{(1-\cosh\alpha_m+\sinh\alpha_m)}{m\pi}\right] + a\sum_m A_m\left[\tanh\alpha_m - \frac{1}{m\pi}\left(1-\frac{1}{\cosh\alpha_m}\right)\right] - \frac{2a}{\pi}\sum_m B_m \frac{(-1)^{\frac{m-1}{2}}}{m}\tanh\beta_m\left[(-1)^{\frac{m-1}{2}}\frac{m\pi}{2}-1\right], \tag{37}$$

The Central Deflection:

$$w = \frac{P_z a^2}{2\pi^3 D}\sum_m \frac{1}{m^3}\left(\tanh\alpha_m - \frac{\alpha_m}{\cosh^2\alpha_m}\right) + \frac{a^2}{2\pi^2 D}\sum_m A_m \frac{(-1)^{\frac{m-1}{2}}}{m^2\cosh\alpha_m}(\alpha_m\tanh\alpha_m) + \frac{2a^2}{\pi^2 D}\sum_m B_m \frac{(-1)^{\frac{m-1}{2}}}{m^2\cosh\beta_m}(\beta_m\tanh\beta_m). \tag{38}$$

The computations outlined above were programmed on the CDC 3400 Computer at Kaman Nuclear. The storage capacity of the computer has dictated the maximum matrix size for A_m and B_m. The matrix size used was 148×148, meaning that 74 of each could be calculated. Inasmuch as the terms in the series were of alternating sign, a matrix of size 146×146 was also solved and the values of displacement and reactions compared for convergence. Table 1 lists the calculated reactions determined from the finite difference analysis and the average of 73 and 74 terms.

Table 1

Quantity	73 coefficients	74 coefficients	Average	Finite difference solution
Central deflection (38)	$0.00723\frac{P_z a^2}{D}$	$0.00723\frac{P_z a^2}{D}$	$0.00723\frac{P_z a^2}{D}$	$0.00794\frac{P_z a^2}{D}$
R_x (35)	$0.249032\ P_z$	$0.246867\ P_z$	$0.247950\ P_z$	$0.248\ P_z$
R_y (36)	$0.004117\ P_z$	$0.004116\ P_z$	$0.004117\ P_z$	$0.004\ P_z$
M_{1y} (32)	$0.070471\ P_z a$	$0.070464\ P_z a$	$0.070468\ P_z a$	$0.068\ P_z a$
M_{2x} (33)	$0.061107\ P_z a$	$0.061107\ P_z a$	$0.061107\ P_z a$	$0.061\ P_z a$
M_{3y} (35)	$0.006606\ P_z a$	$0.006606\ P_z a$	$0.006606\ P_z a$	$0.007\ P_z a$
T (37)	$0.092353\ P_z a$	$0.092344\ P_z a$	$0.092349\ P_z a$	$0.088\ P_z a$

Note: R_x R_y represent the integral of shear forces along clamped edges; M_{1y} M_{2x} M_{3y} represent the integrals of moments along clamped edges. T represents the integrals of torsional moment along the edges. Numbers in parenthesis indicate equations used to obtain analytical solutions of the quantities.

The comparison of the finite difference solutions with the closed form analytical solutions indicate extremely small discrepancies except on the case of central deflection where the error is on the order of 10%. Using finer network in obtaining stiffness coefficients by finite difference method even this discrepancy can be eliminated. It is desirable to use the stiffness coefficients based upon the closed form solution or finer network, especially when limited storage capacity of the computer limits the order of stiffness matrix seriously. In case of distributed loads, however, larger number of discrete elements are mandatory in order to be able to effectively replace distributed loads by concentrated loads acting at the node points.

The stiffness coefficients given in Fig. 10 are based on finite difference solutions. As the numerical example (Fig. 21) illustrates, the rapid convergence of the solution even in case of coarse subdivision, assures the accuracy conventionally required in structural design ($\pm 5\%$).

As a second check on the finite difference solution, a relatively good approximation to the actual deflection surface can be obtained by a double Fourier series in the form of:

$$w = \tfrac{1}{4} \sum_m \sum_n \overline{W}_{mn} \left(1 - \cos \frac{m \pi x}{a}\right) \cdot \left(1 - \cos \frac{2 n \pi y}{b}\right), \tag{39}$$

where $\overline{W}_{mn}$ is computed from the Galerkin's solution of the problem, by expressing the total virtual work in form of:

$$\iint \left(\nabla^4 w - \frac{P_z}{D}\right) \delta w \, dx \, dy. \tag{40}$$

The elements of the siffness matrix of the discrete plate element are tabulated in Fig. 10. The sign convention is as shown in Fig. 3; i.e., all translations are positive if they are in the direction of the positive coordinate axes, and all rotations are positive when they follow the positive rotations shown in Fig. 3. The same sign convention is valid for external and internal forces. Needless to say, since the computation of the stiffness coefficients for the discrete element has been completed, the results (Fig. 10) are reusable for other plate problems without repeating the tedious work of computing these factors.

One of the most important advantages of the stiffness matrix approach to the solution of complex plate problems is that any physically possible boundary condition can be handled with ease.

Thus far, all possible motions of the node points of the discrete element have been considered, resulting in a 12×12 matrix. In the case that one of the node points is prevented from executing all three motions (translation in the Z direction, rotations around X and Y axis) by the boundary condition, the matrix shown in Fig. 10 must be deflated by deleting the columns and rows which corresponds to the numbering of the motions which can not take place. Failing this, the determinant of the stiffness matrix of the total structure will be zero; consequently, the inverse of the matrix is undefined.

	1	2	3	4	5	6	7	8	9	10	11	12
1	$\frac{31.487}{a^2}$											
2	$\frac{-15.617}{a^2}$	$\frac{31.487}{a^2}$										
3	$\frac{-0.252}{a^2}$	$\frac{-15.617}{a^2}$	$\frac{31.487}{a^2}$				Symmetric					
4	$\frac{-15.617}{a^2}$	$\frac{-0.252}{a^2}$	$\frac{-15.617}{a^2}$	$\frac{31.487}{a^2}$								
5	$\frac{-4.282}{a}$	$\frac{3.871}{a}$	$\frac{0.441}{a}$	$\frac{3.871}{a}$	4.041							
6	$\frac{-3.871}{a}$	$\frac{4.282}{a}$	$\frac{-3.871}{a}$	$\frac{-0.441}{a}$	0.592	4.041						
7	$\frac{-0.441}{a}$	$\frac{-3.871}{a}$	$\frac{4.282}{a}$	$\frac{-3.871}{a}$	0.175	−0.592	4.041					
8	$\frac{3.871}{a}$	$\frac{0.441}{a}$	$\frac{3.871}{a}$	$\frac{-4.282}{a}$	−0.592	0.175	0.592	4.041				
9	0	$\frac{5.542}{a}$	0	$\frac{-5.542}{a}$	0	0.817	0	0.817	4.945			
10	$\frac{-5.542}{a}$	0	$\frac{5.542}{a}$	0	0.817	0	0.817	0	1.356	4.945		
11	0	$\frac{5.542}{a}$	0	$\frac{-5.542}{a}$	0	0.817	0	0.817	−0.005	−1.356	4.945	
12	$\frac{-5.542}{a}$	0	$\frac{5.542}{a}$	0	0.817	0	0.817	0	−1.356	−0.005	1.356	4.945

$\cdot D$

Fig. 10. Stiffness matrix of discrete element based on finite difference solution

For instance, if node point "*D*" is completely fixed, rows and columns corresponding to the prevented motions (motions No. 4, 8, 12, Fig. 1) must be deleted from the stiffness matrix shown in Fig. 10. If node "*D*" is freely supported, then only its translation in the Z direction (motion No. 4) and its rotation around the X axis (motion No. 12) is prevented by the support; thus, only the 4th and 12th columns and rows of the stiffness matrix will be eliminated.

Elastic supports and elastic restraints are treated by adding, algebraically, the stiffness factors (spring constants) of the elastic supports to the corresponding elements of the stiffness matrix; thus:

$$\rho_{ij} = \rho_{ij} + \rho_{ij}^{\mathrm{I}} + \rho_{ij}^{\mathrm{II}} + \cdots \tag{41}$$

The consideration of arbitrary geometrical boundaries creates some geometrical fitting problems, since square elements can approximate irregular shapes only by reducing size (mosaic effect) which has an adverse effect on the economy of the solution.

The most effective way to cope with boundaries of arbitrary shape is to introduce additional discrete elements in the form of isosceles triangles Fig. 11. Work concerning this solution has been started by the senior author. In the meantime, the following approximation is recommended along with reduction of the size of the discrete elements to half ($=a/2$) of the square elements used outside of boundaries of irregular shape. The trapezoidal edge element (Fig. 12) is transformed into an equivalent square plate having the same area as that of the trapezoid. Care must be taken that the nodal points near the edges coincide [18].

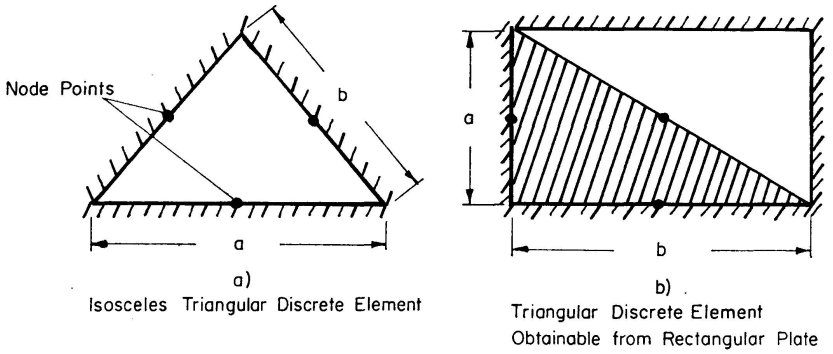

Fig. 11. Triangular discrete elements.

The consideration of stiffeners (or edge beams) merely requires the algebraic addition of stiffness factors of the stiffeners to the corresponding stiffness elements of the discrete elements (Eq. 41). The development of stiffness matrices of beam elements consisting of flanges joined by webs is based on the assumption that the flanges carry axial stresses while the web carries shear stresses, as shown in Fig. 13. The required stiffness matrix elements are easily derived

from conventional beam theory; consequently, their discussion will be negelcted with reference to the pertinent literature [11], [15].

Orthotropic plates are gaining considerable importance in bridge design and are widely used in aerospace and marine structures. In case orthotropy is caused by large, widely spaced stiffners (or floor beams), the above described method, utilizing "disassembled structures", must be used. Orthotropic plates, which have closely spaced small stiffners (or corrugation) (Fig. 14), may be

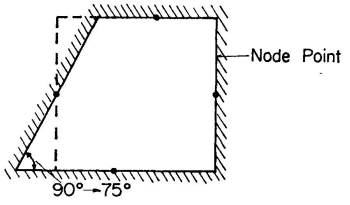

Fig. 12. Approximation of trapezoidal discrete element.

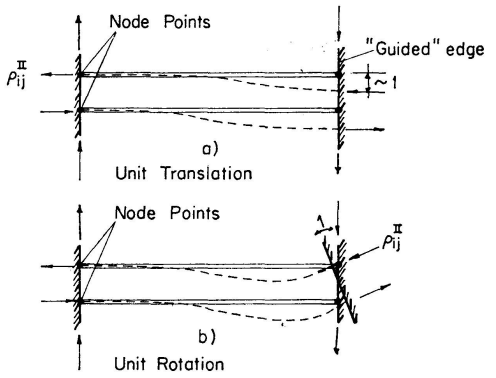

Fig. 13. Development of stiffness matrices of beam elements.

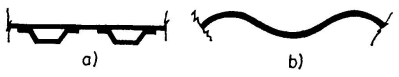

Fig. 14. Orthotropic plates.

approximated by an equivalent isotropic plate which has the flexural rigidity [17]:

$$D_e \cong 2\,(G\,I)_{xy} + \tfrac{1}{2}\,\mu_x D_y + \mu_y D_x, \tag{42}$$

where:

$$D_x = \frac{E_x I_x}{1-\mu_x \mu_y} \quad \text{and} \quad D_y = \frac{E_y I_y}{1-\mu_x \mu_y}, \tag{43}$$

D_x and D_y represent the flexural rigidities in X and Y directions, respectively, I_x and I_y denote the moments of inertia in the two main directions, $2\,(G\,I)_{xy}$ is the average torsional rigidity.

Furthermore, it is evident that the discrete element approach presented in this paper permits the consideration of variable plate thicknesses requiring merely the change of the flexural rigidity (Eq. (13) and Fig. 10) in computing the elements of the stiffness matrix of the discrete element.

IV. Compilation of Stiffness Matrix and its Automation

After determining the elements of the stiffness matrix of the individual discrete elements, the next step is to compile them into the stiffness matrix of the whole plate. Whether this step is done manually or by means of electronic computers as described later, the following simple rules must be followed:

1. Replace all distributed loads by concentrated loads acting at node points only. In case of dynamic problems, the lumped masses must be assigned to the node points.
2. Follow the sign convention shown in Fig. 3 for all external forces and motions.
3. Indicate and number all possible motions (n) of the node points following a convenient sequence. Do not assign numbers to motions which cannot take place in spite of the fact that reactions are produced at those points.
4. Assign the same number, in form of subscript, to the external forces and moments (including inertia forces) which corresponds to the direction of motion the force or moment creates.
5. Number the elements of the stiffness matrices of the individual discrete elements using the same numbering system as used for the motions, but using two indices. The first subscript indicated the "direction"; the second, the "cause" of the force (= stiffness factor). Thus, ρ_{ij} represents a stiffness coefficient in the direction "i" produced by the motion "j".
6. Compile the stiffness matrix by placing the elements as prescribed by the subscripts. Add overlapping elements algebraically (Fig. 15).
7. Invert stiffness matrix by computer.

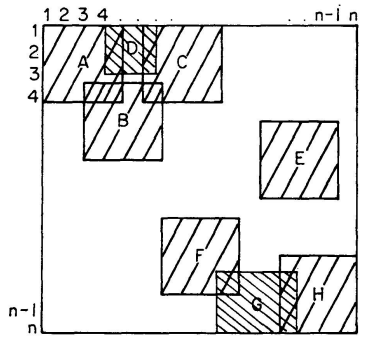

Fig. 15. Partially assembled stiffness matrix of a plate.

The elements of the stiffness matrices of individual elements can easily be placed into the stiffness matrix for the entire plate without resorting to a tedious element-by-element input approach since their location is prescribed by their subscripts (i, j). A flow chart showing compilation of stiffness matrix by computer is shown in Fig. 16. Fig. 17 shows a flow chart for forced vibration solution (Eq. (4)).

V. Numerical Examples

In order to obtain information concerning the degree of accuracy, convergence, effort required, etc., of the method presented in this paper, the plate shown in Fig. 18 has been analyzed for static and dynamic conditions and the results compared with known analytical solutions.

For static loading conditions, the simply supported square plate was

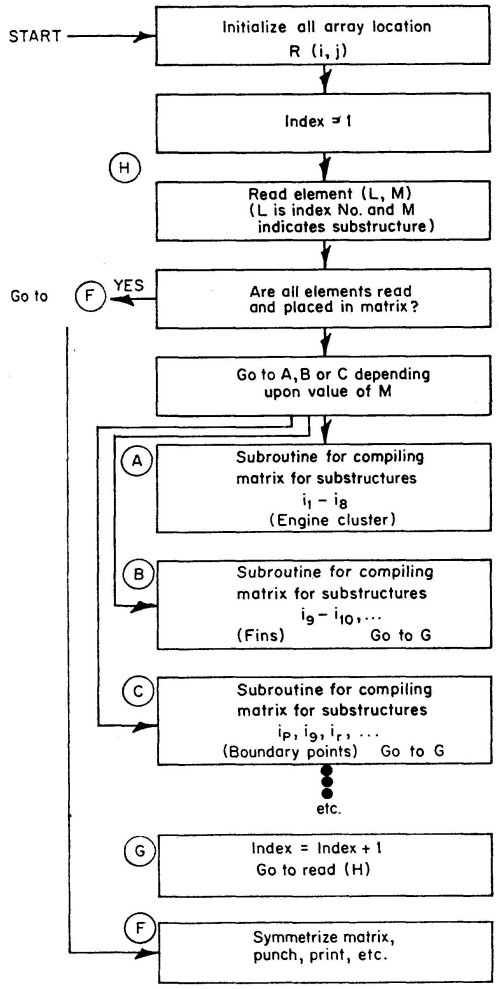

Fig. 16. Flow chart for compilation of stiffness matrix.

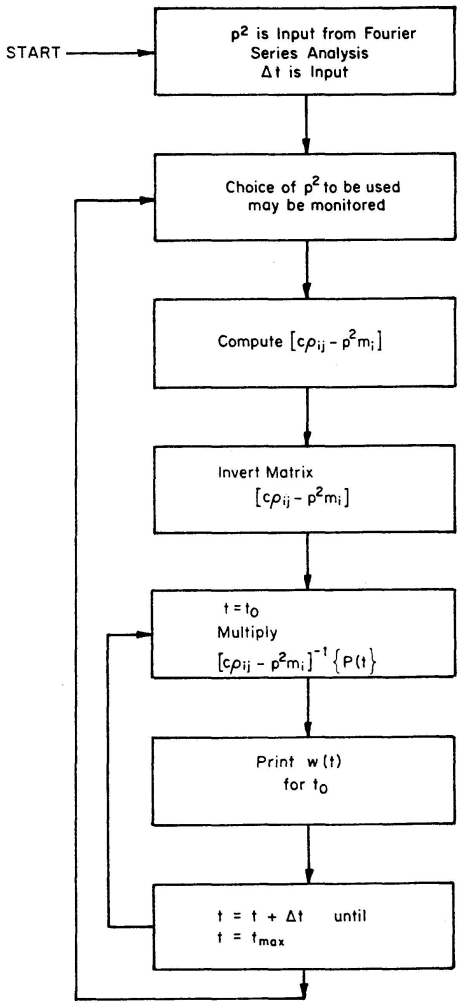

Fig. 17. Flow chart for forced vibration computation.

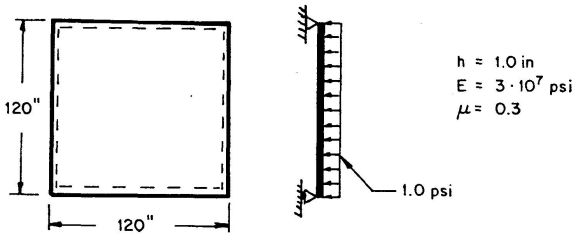

Fig. 18. Numerical example for static loading.

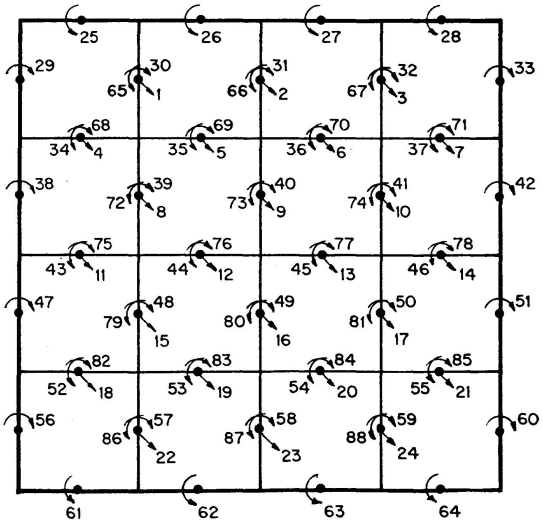

Fig. 19. Numbering of motions for 4×4 element analysis.

subjected to $p_z = 1.0$ psi uniformly distributed load and the deflection surface calculated using 2×2, 3×3, 4×4 and 5×5 discrete element subdivision.

Fig. 19 shows the numbering of the motions for the $4 \times 4 = 16$ element analysis. The corresponding stiffness matrix is shown in Fig. 20. The detailed matrix expression of Eq. (5) has the following form:

$$\begin{bmatrix} w_1 \\ w_2 \\ \vdots \\ w_n \\ \theta_1 \\ \theta_2 \\ \vdots \\ \theta_n \\ \phi_1 \\ \phi_2 \\ \vdots \\ \phi_n \end{bmatrix} = [\rho_{ij}] \begin{bmatrix} P_1 \\ P_2 \\ \vdots \\ P_n \\ M_1 \\ M_2 \\ \vdots \\ M_n \\ T_1 \\ T_2 \\ \vdots \\ T_n \end{bmatrix}, \tag{44}$$

where w_i represents vertical translation, θ_i rotation caused by bending moment, and ϕ_i rotation produced by torque.

The results of the improved matrix solutions are shown in Fig. 21 including the rapid convergence tendency as the number of discrete elements are increased.

The matrix solution has been compared with the analytical solution given in form of double Fourier series:

$$w(x, y) = \frac{16\, p_z}{\pi^2 D} \sum_{m}^{\infty} \sum_{n}^{\infty} \frac{\sin \frac{m \pi x}{a} \sin \frac{n \pi y}{b}}{mn \left(\frac{m^2}{a^2} + \frac{n^2}{b^2} \right)}. \tag{45}$$

The deflections calculated, using the first four terms of the series, are:

$$\text{at} \quad \frac{a}{8}; \quad w = 0.122531 \text{ in}, \qquad \frac{a}{3}; \quad w = 0.268414 \text{ in}, \qquad \frac{3a}{8}; \quad w = 0.285046 \text{ in}. \tag{46}$$

The comparison of these values with the ones obtained by matrix analysis is also illustrated in Fig. 21. This comparison shows that the proposed matrix analysis is rapidly converging to the correct value and finer subdivision reduces the error to negligible proportions.

The time and effort required to compile the matrix by hand for a 4×4 element analysis is approximately 30 minutes; the total time for compiling and computing on the CDC 3400 Computer is approximately 2 minutes, illustrating the economy of the method. This economy is even more pro-

	1	2	3	4	5	6	7	8	9	10	11	12
1	0.096114											
2	−0.047671	0.096114										
3	−0.000769	−0.047671	0.096114			Symmetric						
4	−0.047671	−0.000769	−0.047671	0.096114								
5	−0.392125	0.354487	0.040385	0.354487	11.101648							
6	−0.354487	0.392125	−0.354487	−0.040385	1.626374	11.101648						
7	−0.040385	−0.354487	0.392125	−0.354487	0.480769	−1.626374	11.101648					
8	0.354487	0.040385	0.354487	−0.392125	−1.626374	0.480769	1.626374	11.101648				
9	0.000000	0.507509	0.000000	−0.507509	0.000000	2.244505	0.000000	2.244505	13.585165			
10	−0.507509	0.000000	0.507509	0.000000	2.244505	0.000000	2.244505	0.000000	3.725275	13.585165		
11	0.000000	0.507509	0.000000	−0.507509	0.000000	2.244505	0.000000	2.244505	−0.013736	−3.725275	13.585165	
12	−0.507509	0.000000	0.507509	0.000000	2.244505	0.000000	2.244505	0.000000	−3.725275	−0.013736	3.725275	13.585165

All numbers 10^6

Fig. 20. Stiffness matrix of discrete element of 4×4 element analysis.

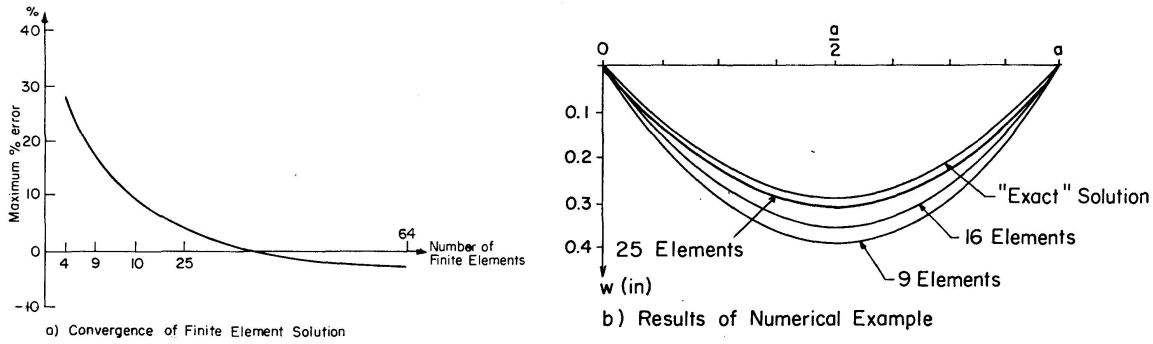

Fig. 21. Results of numerical example.

nounced in the case of arbitrary boundary conditions coupled with arbitrary loading, when automation in compiling the stiffness matrix is applied.

For dynamic analysis, the lowest natural frequencies of the same plate (Fig. 18) were computed using the CDC 3400 Computer and compared with the known results: [17], (21):

$$\omega_1 = \frac{2\pi^2}{a^2}\sqrt{\frac{g\,D}{\gamma\,h}}, \quad \text{(rad/sec)} \tag{47}$$

where ω_1 is the natural circular frequency of the first fundamental mode of vibration, g is the gravitational acceleration, and γ weight density (#/in³).

The comparison of values obtained from Eq. (33), and from the eigen-value of the 4×4 element (Eq. (7)):

$$\omega_{exact} = 13.0\,\text{cps}; \qquad \omega_{matrix} = 13.3\,\text{cps}$$

shows an error of 2.3% which reaches a negligible value by increasing the number of subdivisions [2]).

Besides the demonstrated accuracy and economy of the described matrix approach, its expandability to solve related problems such as thin shells is illustrated by the senior author in [20]. In addition to the previously mentioned extension by determining the stiffness matrix of triangular plate elements, the senior author expects to investigate the effects of single and double curvatures on the elements of the stiffness matrix of square discrete elements, including membrane and bending theories.

The mass matrix was computed according to Reference [6], pp. 176.

Furthermore it is important to remember that the theoretical results are approached from the "lower bound". Since the computed stiffness of the plate is somewhat larger than the actual one, the solution converges to a slightly smaller deflection than obtained by rigorous solution (Fig. 21a).

---

[2]) Error in frequencies corresponding to the second and third modes of free vibrations is below 10%.

VI. Acknowledgement

The authors are indebted to the University of Denver and to Kaman Nuclear for generous donation of their computer and publishing facilities. They also aknowledge the preparation of flow charts by Mrs. Anita West, Research Mathematician.

VII. References

1. QUINLAN, P. M.: "Linear Boundary-Value Problems, the Lambda Method for Polygonal Plates." AFOSR, April, 1964.
2. TIMOSHENKO, S. and WOINOWSKY-KRIEGER, S.: "Theory of Plates and Shells." McGraw-Hill Book Co., New York, 1959.
3. HUBKA, W. F.: "Analysis of Plates of Arbitrary Shape and Boundary Condition." A thesis (M. S.) presented to the Faculty of the College of Engineering, University of Denver, Denver, Colorado, March, 1965.
4. GIRKMANN, K.: «Flächentragwerke.» Springer-Verlag, Wien, 1959.
5. MCMINN, S. J.: "Matrices for Structural Analysis." John Wiley and Sons, Inc., New York, 1962.
6. HURTY, W. C. and RUBINSTEIN, M. F.: "Dynamics of Structures." Prentice-Hall, Inc. Englewood Ciffs, N. J. 1964.
7. ZURMÜHL, R.: «Matrizen.» Springer-Verlag, Berlin, 1961.
8. FRANKLIN, PH.: "An Introduction to Fourier Methods and Laplace Transformation." Dover Publications, Inc., New York, 1958.
9. ARGYRIS, J. H. and KELSEY, S.: "Modern Fusilage Analysis and the Elastic Aircraft." Butterworth, London, 1963.
10. KERSTEN, R.: «Das Reduktionsverfahren der Baustatik.» Springer-Verlag, Berlin, 1962.
11. ARCHER, T. S.: "Digital Computation for Stiffness Matrix Analysis." Journal of the Structural Division, Proceedings ASCE, Oct. 1958.
12. HRENNIKOFF, A.: "Solution of Problems of Elasticity by the Framework Method." Journal of Applied Mechanics, Dec. 1941.
13. MELOSH, R. J.: "A Stiffness Matrix for the Analysis of Thin Plates in Bending." Journal of the Aerospace Sciences, Jan. 1961.
14. HESSEL, A.: "Analysis of Plates and Shells by Matrix Methods." JAAB Report TN-4 B.
15. TURNER, M. T., CLOUGH, R. W., MARTIN, H. C., and TOPP, T.: "Stiffness and Deflection Analysis of Complex Structures." Journal of Aeronautical Sciences, Vol. 25, Sept. 1956.
16. STIGLAT, K.: «Rechteckige und schiefe Platten mit Randbalken.» Wilhelm Ernst & Sohn, Berlin, 1962.
17. WAH, I.: "A Guide for the Analysis of Ship Structures." U. S. Department of Commerce, Washington, D. C., 1960.
18. PUCHER, A.: «Einflußfelder elastischer Platten.» Springer-Verlag, Wien, 1951.
19. HOELAND, G.: «Stützenmomenten-Einflußfelder durchlaufender Platten.» Springer-Verlag, Berlin, 1957.
20. SZILARD, R.: "A Matrix and Computer Solution of Cylindrical Shells of Arbitrary Shape." Pager presented at the International Sumposium on Shell Structures in Engineering Practice, held in Budapest, Aug. 31—Sept. 3, 1965.
21. TIMOSHENKO, S.: "Vibration Problems in Engineering." D. Van Nostrand Co., Inc. Princeton, N. J., 1959.

Summary

An improved stiffness matrix solution of complex static and dynamic plate problems is presented. For discrete elements, square plates have been introduced. The nodal points where continuity is expressed are located at the center of the fixed edges of the discrete elements. The node points, subjected to unit motions, produce the required elements of the stiffness matrix, which are obtained by solving the differential equation of the plate by various methods. The accuracy and economy of the method has been demonstrated by numerical examples. The possibility of more or less complete automation of the procedure is outlined.

Résumé

Les auteurs présentent une solution améliorée pour l'étude, à l'aide d'une matrice de rigidité, de problèmes de plaques compliqués, tant statiques que dynamiques. Les éléments de base sont des carrée avec, au milieu des côtés encastrés, les nœuds où sont remplies les conditions de continuité. En soumettant ces nœuds à des déplacements unitaires, on obtient les éléments de la matrice de rigidité en résolvant par diverses méthodes l'équation différentielle des plaques. Des applications numériques montrent la précision et l'économie de la méthode. Pour l'utilisation, on peut pousser l'automation plus ou moins loin.

Zusammenfassung

Eine verbesserte Lösung der Steifigkeitsmatrix für komplexe statische und dynamische Plattenprobleme wird dargestellt. Als Grundelemente wurden quadratische Platten eingeführt. Die Knotenpunkte, an denen die Kontinuität ausgedrückt wird, befinden sich in der Mitte der eingespannten Ränder der Grundelemente. Durch Einheitsbewegungen der Knotenpunkte werden die erforderlichen Elemente der Steifigkeitsmatrix ausgedrückt, welche durch die Auflösung der Differentialgleichungen der Platte erhalten werden. Die Genauigkeit und Wirtschaftlichkeit der Methode wird anhand von numerischen Beispielen gezeigt. Die Möglichkeit einer mehr oder weniger weitgehenden Automatisierung des Verfahrens wird skizziert.